Quantum Electronics **31** (9) 804 – 810 (2001)

INTERACTION OF LASER RADIATION WITH MATTER. LASER PLASMA

PACS numbers: 52.25.Os; 52.38.–r
DOI: 10.1070/QE2001v031n09ABEH002049

Conversion of electromagnetic waves at the ionisation front

M V Chegotov

***Abstract*. It is shown that a weak electromagnetic pulse interacting with a copropagating ionisation front is converted in the general case into three electromagnetic pulses with higher and lower frequencies, which propagate in different directions. The coefficients of conversion to these pulses (for intensities) were found as functions of the frequency. The electromagnetic energy is shown to decrease during this conversion because of the losses for the residual electron energy.**

Keywords: *ionisation front, conversion coefficient, residual energy.*

1. Introduction

A wealth of papers were concerned with the interaction of electromagnetic radiation with a plasma whose spatiotemporal density profile travels with a velocity close to the speed of light (see, e.g., Refs [1 – 12]). This interest is caused both by the possibilities of increasing the laser radiation frequency and, for instance, by the use of frequency change of ultrashort laser pulses upon the interaction with travelling plasma density profiles to analyse the laser–plasma interaction (see, for instance, Ref. [13]). Note that the statements of the problem of increasing the electromagnetic radiation frequency in Refs [1 – 4] and Refs [5 – 12] are significantly different: in Refs [1 – 4], the frequency of electromagnetic waves increases upon their reflection from the plasma boundary which travels towards the electromagnetic radiation, whereas in Refs [5 – 12] the interaction of copropagating electromagnetic radiation and plasma profile is considered.

In this paper, the interaction of a copropagating ionisation front and a weak electromagnetic pulse is studied. The approximation of slowly varying amplitudes underlies the consideration of this interaction in the overwhelming majority of papers (in view of the nonlinear nature of the interaction between the laser radiation and the ionisation front, this approximation was termed quasi-harmonic in Ref. [6]). The frequency assigned to laser radiation in the context of this approximation proves to be the function of position on the travelling time profile of the laser pulse. This frequency mainly varies in the vicinity of strongest gradients of the plasma electron density profile, which travels in the same direction as the laser pulse. The frequency variations may be quite significant for a relatively long interaction between the laser pulse and a copropagating density gradient.

However, within the above local approach to the definition of laser radiation frequency, a question remains as to what is the frequency spectrum of the laser pulse after its escape from the interaction region (from the plasma). Furthermore, calculations performed by the particle-in-cell method showed that quasi-harmonic description of the interaction between the laser radiation and the ionisation front is inadequate [12]. Indeed, the results of the one-dimensional calculation of Ref. [12] imply that the spectrum of a laser pulse turns out to be split after its passage through the gas: one part of the spectrum is blue-shifted from the initial main spectral component of the laser pulse at entry to the gas, and the other is red-shifted. The intensity of the red satellite may be higher or lower than the intensity of the blue one, depending on the pulse penetration depth in the gas. The quasi-harmonic approximation does not take into account the simultaneous existence of these two frequency components.

We will consider the interaction of a low-intensity pulse (weak pulse) with a copropagating ionisation front in a one-dimensional geometry employing an approximation linear in the field of the weak pulse. The origin of the ionisation front is of no significance; however, here it will be assumed to arise from the ionisation of gas by an intense laser pulse. In this case, the ionisation-front profile will be assumed to be stationary and its velocity to be equal to the group velocity of propagation of the intense laser pulse in the plasma being produced by this pulse.

Upon the interaction of the ionisation front with a weak pulse, the latter splits in the general case into three pulses: (1) the pulse transmitted through the ionisation front, whose frequencies ω_t for a low gas density are significantly higher than the characteristic frequencies ω of the initial weak pulse; (2) the delayed pulse, whose frequencies ω_r^s do not exceed the characteristic frequencies of the ionising pulse and which propagates in the same direction as the ionisation front, though with a lower velocity; and (3) the reflected pulse (with frequencies ω_r^b), which propagates in the opposite direction relative to the front propagation.

M V Chegotov Institute for High Energy Densities, Joint Institute of High Temperatures, Russian Academy of Sciences, Izhorskaya ul. 13/19, 127412 Moscow, Russia;
e-mail: chegotov@hedric.msk.su

Received 20 April 2001
Kvantovaya Elektronika **31** (9) 804 – 810 (2001)
Translated by E N Ragozin

It follows from the relationships between the spectral intensity densities of these three pulses $[I_t(\omega_t), I_r^s(\omega_r^s), I_r^b(\omega_r^b)]$ and the spectral intensity density $I(\omega)$ of the initial pulse, in particular, that the weak-pulse conversion coefficients (for the spectral intensity densities) to the frequency components of the transmitted (ω_t), delayed (ω_r^s), and reflected (ω_r^b) pulses depend substantially on the shape of the ionisation front. Namely, when the front is smooth and long enough, the maximum coefficient (as a function of the frequency ω_t) of conversion to the transmitted pulse is significantly higher than unity, whereas the coefficient of conversion to the delayed pulse does not exceed unity and decreases with decreasing frequency (see below, for instance, Fig. 3).

Therefore, when some frequency component ω passes through the ionisation front, there occurs an increase not only in its frequency (from ω to ω_t), but also in its spectral intensity density $I_t(\omega_t)$ in comparison with $I(\omega)$.Despite this increase, the total energy of its daughter pulses in this case proves to be lower than the initial pulse energy. This decrease is caused by the energy losses of the initial pulse due to the residual energy.

2. Basic equations

Consider a layer of a neutral gas whose density n_{at} is uniform along the x and y axes but nonuniform along the z axis. We assume that the density $n_{at}(z)$ is constant over a length L_g and decreases to zero on either side of the nonuniform layer on scales significantly exceeding the characteristic wavelengths of the electromagnetic waves in this problem. The intense ionising electromagnetic pulse is incident from the region $z = -\infty$. The weak pulse is also incident from the region $z = -\infty$ and has an initial (outside of the gas) spectral intensity density $I(\omega)$.

We also assume that, first, the ionising pulse in the region $z = -\infty$ is ahead of the weak pulse, so that the latter reaches the ionisation front in the region of already initially uniform gas and, second, the most intense part of the weak pulse has enough time to interact with the ionisation front over the length L_g. The second assumption implies, in particular, that the length L_g should be long enough: $L_g > L_p V/(V_{ph} - V)$, where L_p is the characteristic length of the weak pulse; V_{ph} is its phase velocity; V is the velocity of the ionisation front. Assuming that the ionisation front is stationary, we obtain that the electron density profile n_e is a function of only the coordinate $\zeta = z - Vt$ co-moving with the ionisation front.

The electric field of the weak pulse $\boldsymbol{E}(\zeta, \tau)(\tau = t)$, polarised along the x axis ($\boldsymbol{E} = \boldsymbol{e}_x E$), obeys the wave equation in the coordinates z and t of the laboratory frame of reference (j_x is the projection of free-electron current density on the x axis):

$$\frac{1}{c^2}\frac{\partial^2 E}{\partial t^2} - \frac{\partial^2 E}{\partial z^2} + \frac{4\pi}{c^2}\frac{\partial j_x}{\partial t} = 0\,.$$

In the co-moving coordinates $\zeta = z - Vt$ and $\tau = t$, the wave equation has the form

$$\frac{1}{c^2}\frac{\partial^2 E}{\partial \tau^2} - \frac{2V}{c}\frac{\partial^2 E}{\partial \zeta\, \partial \tau} - \left(1 - \frac{V^2}{c^2}\right)\frac{\partial^2 E}{\partial \zeta^2} + k_p^2(\zeta)E = 0, \qquad (1)$$

where $k_p^2(\zeta) = \omega_p^2(\zeta)/c^2 = 4\pi e^2 n_e(\zeta)/(mc^2)$; m and e are the electron mass and charge; and c is the velocity of light. Eqn (1) follows from the equation for the current density $\boldsymbol{j}$ of the free electrons produced due to ionisation of the material by the intense laser pulse, which oscillate under the action of the weak-pulse electric field $\boldsymbol{E}$:

$$\frac{\partial \boldsymbol{j}}{\partial t} = \frac{e^2 n_e}{m}\boldsymbol{E}. \qquad (2)$$

Eqn (1) for the Fourier transform E_Ω of the field E $[E_\Omega(\zeta) = \int_{-\infty}^{+\infty} E(\zeta, \tau)\exp(i\Omega\tau)\,d\tau]$ takes the form

$$\frac{\partial^2 E_\Omega}{\partial \zeta^2} - \frac{2i V\Omega}{c^2 - V^2}\frac{\partial E_\Omega}{\partial \zeta} + \frac{\Omega^2}{c^2 - V^2}E_\Omega = \frac{\omega_p^2(\zeta)}{c^2 - V^2}E_\Omega.$$

By using this equation, we derive the equation for the function $\tilde{E}_\Omega(\zeta) = E_\Omega(\zeta)\exp[i\Omega V\zeta/(c^2 - V^2)]$:

$$\frac{\partial^2 \tilde{E}_\Omega}{\partial \zeta^2} + \frac{c^2\Omega^2}{(c^2 - V^2)^2}\left[1 - \left(1 - \frac{V^2}{c^2}\right)\frac{\omega_p^2(\zeta)}{\Omega^2}\right]\tilde{E}_\Omega = 0. \qquad (3)$$

Eqn (3) should be supplemented with boundary conditions. They follow from the spatiotemporal evolution of the electron density n_e, which is constant outside of the ionisation front:

$$n_e(\zeta) = \begin{cases} n_{e\max}, & \zeta \to -\infty, \\ 0, & \zeta \to +\infty. \end{cases}$$

According to our formulation of the problem, the weak pulse is incident on the ionisation front from the region of the ionised gas ($\zeta \to -\infty$), and therefore

$$\tilde{E}_\Omega(\zeta) = \begin{cases} \tilde{E}_{0\Omega}\exp[iK(\Omega)\zeta] + \tilde{E}_{r\Omega}\exp[-iK(\Omega)\zeta], & \zeta \to -\infty, \\ \tilde{E}_{t\Omega}\exp[ic\Omega\zeta/(c^2 - V^2)], & \zeta \to +\infty, \end{cases} \qquad (4)$$

where

$$K(\Omega) = \left[\frac{\Omega^2}{c^2}\left(1 - \frac{V^2}{c^2}\right)^{-2} - k_{p\max}^2\left(1 - \frac{V^2}{c^2}\right)^{-1}\right]^{1/2};$$

$k_{p\max}^2 = \omega_{p\max}^2/c^2 = 4\pi e^2 n_{e\max}/(mc^2)$; $\tilde{E}_{0\Omega}$ is the incident-wave amplitude; $\tilde{E}_{r\Omega}$ is the amplitude of the wave reflected from the ionisation front; $\tilde{E}_{t\Omega}$ is the amplitude of the wave transmitted through the ionisation front. Note that Ω is the frequency and $\tilde{E}_{0\Omega}$, $\tilde{E}_{r\Omega}$ и $\tilde{E}_{t\Omega}$ are the amplitudes of the waves in the co-moving frame of reference. To go over to the laboratory frame of reference where the ionisation front travels with the velocity V, we will write the field in the region of fully ionised plasma as

$$E^L(z,t) = \frac{1}{2\pi}\begin{cases} \int_0^{+\infty} E_{0\omega}^L e^{-i\omega\{t - [\varepsilon(\omega)]^{1/2}z/c\}}d\omega + \int_0^{+\infty} E_{r\omega_r}^L e^{-i\omega_r t + ik_{rz}(\omega_r)z}d\omega_r + \text{c.c.}, & \zeta \to -\infty, \\ \int_0^{+\infty} E_{t\omega_t}^L e^{-i\omega_t(t - z/c)}d\omega_t + \text{c.c}, & \zeta \to +\infty \end{cases} \qquad (5)$$

where $\varepsilon(\omega) = 1 - \omega_{\mathrm{p\,max}}^2/\omega^2$ is the permittivity of the electron plasma component and $k_{\mathrm{r}z}(\omega_\mathrm{r})$ is the projection of the wave vector of the reflected wave on the z axis, with $k_{\mathrm{r}z}^2(\omega_\mathrm{r}) = \omega_\mathrm{r}^2\varepsilon(\omega_\mathrm{r})/c^2$. By comparing the expressions for E in the laboratory and co-moving frames of reference [expressions (4) and (5), respectively], we obtain the relations between the frequencies of incident (ω), 'reflected' (ω_r), and transmitted (ω_t) waves in these frames of reference, and also the expression for the projection of the wave vector of the 'reflected wave':

$$\Omega = \omega\left\{1 - \frac{V}{c}[\varepsilon(\omega)]^{1/2}\right\}, \tag{6}$$

$$\omega_\mathrm{t} = \omega\left\{1 - \frac{V}{c}[\varepsilon(\omega)]^{1/2}\right\}\left(1 - \frac{V}{c}\right)^{-1}. \tag{7}$$

$$\omega_\mathrm{r} = \omega\left\{1 - 2\frac{V}{c}[\varepsilon(\omega)]^{1/2} + \frac{V^2}{c^2}\right\}\left(1 - \frac{V^2}{c^2}\right)^{-1}, \tag{8}$$

$$k_{\mathrm{r}z} = \frac{\omega}{c}\left\{2\frac{V}{c} - \left(1 + \frac{V^2}{c^2}\right)[\varepsilon(\omega)]^{1/2}\right\}\left(1 - \frac{V^2}{c^2}\right)^{-1}.$$

It follows from the condition that a given pulse is incident on the ionisation front from the left (i.e. from the region $\zeta = -\infty$), which corresponds to $K \geqslant 01$, that the production of reflected and transmitted waves should be considered when the inequality

$$c[\varepsilon(\omega)]^{1/2} > V \tag{9}$$

is fulfilled. Since $c[\varepsilon(\omega)]^{1/2} = V_\mathrm{g}(\omega)$ is the group velocity of the wave with the frequency ω, it is clear that relation (9) expresses the natural condition for the interaction of this wave with the ionisation front: its group velocity should be higher than the propagation velocity of the ionisation front.

The group velocity of the most intense frequency component ω_0 of the ionising pulse will be selected as the velocity propagation V of the ionisation front:

$$V = c[\varepsilon(\omega_0)]^{1/2} = c\left(1 - \omega_{\mathrm{p\,max}}^2/\omega_0^2\right)^{1/2} = c\left(1 - n_{\mathrm{e\,max}}/n_\mathrm{c}\right)^{1/2}, \tag{10}$$

where $n_\mathrm{c} = 4\pi e^2/(m\omega_0^2)$ is the critical electron density for the ω_0 frequency. The condition (9) and the equality (10) determine the frequencies of the waves that interact with the ionisation front:

$$\omega > \omega_0\,. \tag{11}$$

It follows from relation (7) that the frequencies of waves transmitted through the ionisation front satisfy the inequality

$$\omega_\mathrm{t} > \omega_{\mathrm{t\,min}} \equiv \omega_0\left(1 + \frac{V}{c}\right) = \omega_0\left\{1 + c[\varepsilon(\omega_0)]^{1/2}\right\}. \tag{12}$$

The dependence $\omega_\mathrm{t}(\omega)$ is shown in Fig. 1.

The group velocity of reflected waves is defined by the relation $V_\mathrm{gr} = c^2k_{\mathrm{r}z}/\omega_\mathrm{r}$, which is standard for plasmas and can be obtained from expression (8) by direct differentiation with respect to ω:

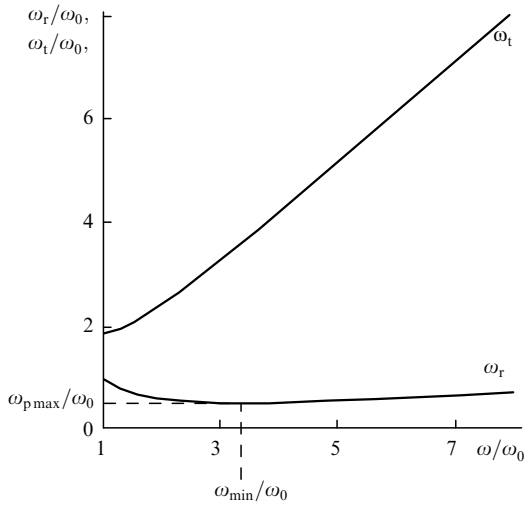

Figure 1. Dependences $\omega_\mathrm{t}(\omega)$ and $\omega_\mathrm{r}(\omega)$ for $n_{\mathrm{e\,max}}/n_\mathrm{c} = 0.25$, which correspond to $\omega_{\mathrm{p\,max}}/\omega_0 = 0.5$ and $\omega_{\mathrm{min}}/\omega_0 = 3.5$.

$$V_\mathrm{gr} = \frac{\mathrm{d}\omega_\mathrm{r}}{\mathrm{d}k_{\mathrm{r}z}} = \frac{\mathrm{d}\omega_\mathrm{r}}{\mathrm{d}\omega}\left(\frac{\mathrm{d}k_{\mathrm{r}z}}{\mathrm{d}\omega}\right)^{-1}.$$

The projection of the wave vector of reflected wave (8) proves to be a sign-variable quantity. Indeed, for $\omega = \omega_0$ it follows from expressions (8) and (10) that $k_{\mathrm{r}z} = \omega_0[\varepsilon(\omega_0)]^{1/2}/c > 0$. For $\omega \to +\infty$, we have $k_{\mathrm{r}z} = -(\omega/c) \times (c - V)/(c + V) < 0$. When the inequality (11) is fulfilled, $k_{\mathrm{r}z}$ changes sign when

$$\omega = \omega_{\mathrm{min}} = \omega_0\frac{\omega_0}{\omega_{\mathrm{p\,max}}}\left(2 - \frac{\omega_{\mathrm{p\,max}}^2}{\omega_0^2}\right), \tag{13}$$

and at the point $\omega = \omega_{\mathrm{min}}$ it turns out that

$$\omega_{\mathrm{r\,min}} = \omega_{\mathrm{p\,max}}. \tag{14}$$

Therefore, the high-frequency components ($\omega > \omega_{\mathrm{min}}$) are reflected from the ionisation front in such a way that they propagate in the laboratory frame of reference in the direction opposite to that of the ionising pulse. In this case, the spectrum of reflected components lies above the plasma frequency: $\omega_\mathrm{r} > \omega_{\mathrm{p\,max}}$ (see Fig. 1). The frequency components that lie in the interval (ω_0, ω_{min}) are reflected from the ionisation front without changing the direction of propagation in the laboratory frame of reference; the reflected-wave frequencies lie in the interval ($\omega_{\mathrm{p\,max}}$, ω_0). In this case, the group velocity is $V_\mathrm{gr} = c[\varepsilon(\omega_\mathrm{r})]^{1/2} < V = c[\varepsilon(\omega_0)]^{1/2}$, and, therefore, the frequency components lying in the (ω_0, ω_{min}) interval slow down upon reflection from the ionisation front.

Equation (3) in combination with the boundary conditions (4) allows us to determine the relation between the amplitudes of incident, reflected, and transmitted waves in the co-moving frame of reference. To determine the relation between these quantities in the laboratory frame of reference, we should define more precisely the expression for the reflected component. According to the above discussion, the waves reflected in the co-moving frame of reference are subdivided in the laboratory frame into reflected, and delayed waves. The former propagate in the direction opposite to the z axis direction [the amplitude $E_{\mathrm{r}\omega_\mathrm{r}}^{\mathrm{Lb}}$, the branch $\omega_\mathrm{r}^\mathrm{b}$ of the

frequency (8) lies in the interval $(\omega_{\mathrm{p}\max}, +\infty)$ and corresponds to $\omega > \omega_{\min}$ (see Fig. 1)]. The latter [the amplitude $E^{\mathrm{Ls}}_{\mathrm{r}\omega_{\mathrm{r}}}$, the branch $\omega^{\mathrm{s}}_{\mathrm{r}}$ of the frequency (8) lies in the interval $(\omega_{\mathrm{p}\max}, \omega_0)$ and corresponds to $\omega_0 < \omega < \omega_{\min}$ (see Fig. 1)] propagates in the z axis direction:

$$\int_0^{+\infty} E^{\mathrm{L}}_{\mathrm{r}\omega_{\mathrm{r}}} \mathrm{e}^{-\mathrm{i}\omega_{\mathrm{r}} t + \mathrm{i}k_{\mathrm{r}z}(\omega_{\mathrm{r}})z} \mathrm{d}\omega_{\mathrm{r}} = \int_{\omega_{\mathrm{p}\max}}^{+\infty} E^{\mathrm{Lb}}_{\mathrm{r}\omega_{\mathrm{r}}} \mathrm{e}^{-\mathrm{i}\omega_{\mathrm{r}}\{t + [\varepsilon(\omega_{\mathrm{r}})]^{1/2} z/c\}} \mathrm{d}\omega_{\mathrm{r}}$$

$$+ \int_{\omega_{\mathrm{p}\max}}^{\omega_0} E^{\mathrm{Ls}}_{\mathrm{r}\omega_{\mathrm{r}}} \mathrm{e}^{-\mathrm{i}\omega_{\mathrm{r}}\{t - [\varepsilon(\omega_{\mathrm{r}})]^{1/2} z/c\}} \mathrm{d}\omega_{\mathrm{r}}. \qquad (15)$$

To take advantage of the results of solution of Eqn (3) in combination with the boundary conditions (4) in the laboratory frame of reference, we employ the following relations:

$$\tilde{E}_{0\Omega} = E^{\mathrm{L}}_{0\omega} (\mathrm{d}\Omega/\mathrm{d}\omega)^{-1},$$

$$\tilde{E}_{\mathrm{t}\Omega} = E^{\mathrm{L}}_{\mathrm{t}\omega_{\mathrm{t}}} (\mathrm{d}\omega_{\mathrm{t}}/\mathrm{d}\omega)(\mathrm{d}\Omega/\mathrm{d}\omega)^{-1}, \qquad (16)$$

$$\tilde{E}_{\mathrm{r}\Omega} = \begin{cases} E^{\mathrm{Ls}}_{\mathrm{r}\omega_{\mathrm{r}}} (\mathrm{d}\omega^{\mathrm{s}}_{\mathrm{r}}/\mathrm{d}\omega)(\mathrm{d}\Omega/\mathrm{d}\omega)^{-1}, & \omega^2_{\mathrm{p}\max}\omega_0^{-1} \leqslant \Omega \leqslant \omega_{\mathrm{p}\max}, \\ E^{\mathrm{Lb}}_{\mathrm{r}\omega_{\mathrm{r}}} (\mathrm{d}\omega^{\mathrm{b}}_{\mathrm{r}}/\mathrm{d}\omega)(\mathrm{d}\Omega/\mathrm{d}\omega)^{-1}, & \Omega \geqslant \omega_{\mathrm{p}\max}. \end{cases} \qquad (17)$$

3. Energy conservation law

From the Maxwell equations for the electric ($\boldsymbol{E} = \boldsymbol{e}_x E$) and magnetic ($\boldsymbol{H} = \boldsymbol{e}_y H$) fields of the weak pulse, we can readily obtain, in view of Eqn (2), the relation

$$\frac{\partial}{\partial z} \int_{-\infty}^{+\infty} \frac{c}{4\pi} EH \mathrm{d}t = -\int_{-\infty}^{+\infty} \frac{\partial n_{\mathrm{e}}}{\partial t} \frac{m V_E^2(z,t)}{2} \mathrm{d}t, \qquad (18)$$

where

$$V_E(z,t) \equiv \frac{e}{m} \int_{-\infty}^{t} E(z,t') \mathrm{d}t'$$

is the nonrelativistic velocity of an electron in the electric field of the weak laser pulse. The right-hand side of expression (18) is the residual energy density (compare, for instance, with the corresponding formula of the 'Basic equations' section in Ref. [14]) acquired by electrons from the weak pulse at the instant of ionisation. This energy transfer is caused by the nonadiabaticity of ionisation.

By integrating (18) with respect to z between the limits $-\infty$ and $+\infty$, we obtain the expression

$$\int_0^{+\infty} I(\omega) \mathrm{d}\omega = \int_{\omega_{\mathrm{t}\min}}^{+\infty} I_{\mathrm{t}}(\omega_{\mathrm{t}}) \mathrm{d}\omega_{\mathrm{t}} + \int_{\omega_{\mathrm{p}\max}}^{+\infty} I^{\mathrm{b}}_{\mathrm{r}}(\omega^{\mathrm{b}}_{\mathrm{r}}) \mathrm{d}\omega^{\mathrm{b}}_{\mathrm{r}}$$

$$+ \int_{\omega_{\mathrm{p}\max}}^{\omega_0} I^{\mathrm{s}}_{\mathrm{r}}(\omega^{\mathrm{s}}_{\mathrm{r}}) \mathrm{d}\omega^{\mathrm{s}}_{\mathrm{r}} + \int_{-\infty}^{+\infty} \int_{-\infty}^{+\infty} \frac{\partial n_{\mathrm{e}}}{\partial t} \frac{m V_E^2(z,t)}{2} \mathrm{d}t \mathrm{d}z, \qquad (19)$$

which gives the energy conservation law for a weak pulse. Note that $I_{\mathrm{t}}(\omega_{\mathrm{t}}), I^{\mathrm{s}}_{\mathrm{r}}(\omega^{\mathrm{s}}_{\mathrm{r}}), I^{\mathrm{b}}_{\mathrm{r}}(\omega^{\mathrm{b}}_{\mathrm{r}})$ and $I(\omega)$ represent the spectral intensity densities outside of the gas layer. To take advantage of relation (16), (17), and (19), the fields $E^{\mathrm{L}}_{0\omega}$, $E^{\mathrm{Ls}}_{\mathrm{r}\omega_{\mathrm{r}}}, E^{\mathrm{Lb}}_{\mathrm{r}\omega_{\mathrm{r}}}$ in the plasma (the field $E^{\mathrm{L}}_{\mathrm{t}\omega_{\mathrm{t}}}$ is located outside the plasma), which appear in expressions (16) and (17), should be related to the incident and reflected fields outside of the gas layer. When the boundaries of the gas layer are smooth enough, it is possible to derive these relations in the geometrical optics approximation, which gives

$$I(\omega) = \frac{c}{8\pi} \left[\varepsilon(\omega)\right]^{1/2} \left| E^{\mathrm{L}}_{0\omega} \right|^2, \quad I^{\mathrm{s}}_{\mathrm{r}}(\omega^{\mathrm{s}}_{\mathrm{r}}) = \frac{c}{8\pi} \left[\varepsilon(\omega^{\mathrm{s}}_{\mathrm{r}})\right]^{1/2} \left| E^{\mathrm{Ls}}_{\mathrm{r}\omega_{\mathrm{r}}} \right|^2,$$

$$I^{\mathrm{b}}_{\mathrm{r}}(\omega^{\mathrm{b}}_{\mathrm{r}}) = \frac{c}{8\pi} \left[\varepsilon(\omega^{\mathrm{b}}_{\mathrm{r}})\right]^{1/2} \left| E^{\mathrm{Lb}}_{\mathrm{r}\omega_{\mathrm{r}}} \right|^2. \qquad (20)$$

In combination with relations (16) and (17), formulas (20) allow one to determine the weak-pulse conversion at the ionisation front, provided the problem (3), (4) is solved.

4. Ionisation front for different polarisations of the intense pulse

4.1 Circularly polarised pulse

We now discuss the ionisation front model. Fig. 2 shows the density profile for the electrons produced due to tunnel ionisation of hydrogen by circularly polarised Gaussian laser pulse with a wavelength of $\lambda_0 = 0.8$ μm, the maximum intensity $I_{\max} = 8.5 \times 10^{16}$ W cm^{-2}, and the FWHM of 52 fs. The calculation was performed taking into account the tunnel ionisation of atoms by the laser-pulse field (see, for instance, Ref. [14]). To simplify the analytical treatment the electron density profile is approximated in the following way:

$$n_{\mathrm{e}}(\zeta) = \begin{cases} n_{\mathrm{e}\max}, & \zeta < 0, \\ n_{\mathrm{e}\max}/\cosh^2(\zeta/a), & \zeta \geqslant 0 \end{cases}. \qquad (21)$$

The result of approximation is given in Fig. 2.

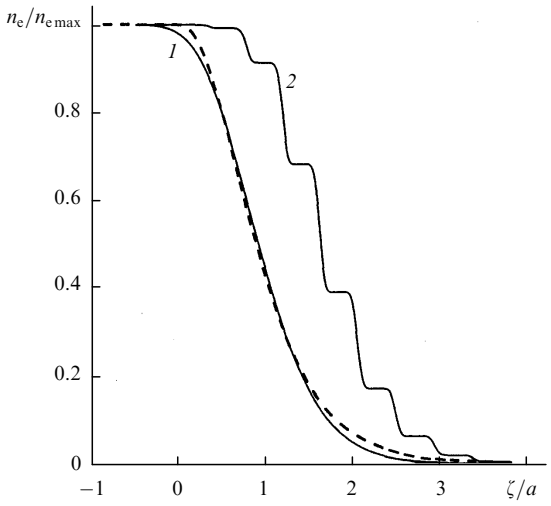

Figure 2. Density profile for the electrons produced upon the tunnel ionisation of hydrogen by circularly (*1*) and linearly polarised (*2*) Gaussian laser pulses with a wavelength $\lambda_0 = 0.8$ μm, a peak intensity $I_{\max} = 8.5 \times 10^{16}$ W cm^{-2}, and a FWHM of 52 fs, and approximation of this profile by the dependence (21) (dashed curve) for $a \approx 0.9$ μm in the case of circularly polarised pulse. The point $\zeta = 0$ corresponds to a laser pulse intensity of $\sim 3.2 \times 10^{14}$ W cm^{-2}.

The solution of Eqn (3) with the electron density profile (21) and the boundary conditions (4) has the form (for $\zeta \geqslant 0$)

$$\tilde{E}_{\Omega}(\zeta) = \tilde{E}_{\mathrm{t}\,\Omega}[4u(1-u)]^{-\mathrm{i}a\Omega c[2(c^2-V^2)]^{-1}} F(\alpha,\beta,\gamma;u), \qquad (22)$$

where $u = [1+\exp(2\zeta/a)]^{-1}$; $F(\alpha,\beta,\gamma;u)$ is the hypergeometric function [15]; $\alpha(\Omega) = 0.5 - \mathrm{i}p(\Omega)a + (0.25 - a^2G)^{1/2}$; $\beta(\Omega) = 0.5 - \mathrm{i}p(\Omega)a - (0.25 - a^2G)^{1/2}$; $\gamma(\Omega) = 1 - \mathrm{i}p(\Omega)a$; $p(\Omega) = (\Omega/c)(1 - V^2/c^2)^{-1}$; $G = k_{\mathrm{p\,max}}^2(1-V^2/c^2)^{-1} = \omega_0^2/c^2$. By sewing together the solution (22) with the boundary condition (4) for $\zeta \leqslant 0$, we obtain

$$\tilde{E}_{\mathrm{t}\Omega} = \frac{2}{\sqrt{\pi}} 2^{-\mathrm{i}a\Omega c/(c^2-V^2)} \times \frac{\Gamma^{-1}[(\alpha+\beta+1)/2]\Gamma[(\alpha+1)/2]\Gamma[(\beta+1)/2]}{1 + \dfrac{2\mathrm{i}}{K(\Omega)a}\dfrac{\Gamma[(\alpha+1)/2]\Gamma[(\beta+1)/2]}{\Gamma(\alpha/2)\Gamma(\beta/2)}} \tilde{E}_{0\Omega}, \qquad (23)$$

$$\tilde{E}_{\mathrm{r}\Omega} = \frac{1 - \dfrac{2\mathrm{i}}{K(\Omega)a}\dfrac{\Gamma[(\alpha+1)/2]\Gamma[(\beta+1)/2]}{\Gamma(\alpha/2)\Gamma(\beta/2)}}{1 + \dfrac{2\mathrm{i}}{K(\Omega)a}\dfrac{\Gamma[(\alpha+1)/2]\Gamma[(\beta+1)/2]}{\Gamma(\alpha/2)\Gamma(\beta/2)}} \tilde{E}_{0\Omega}, \qquad (24)$$

where Γ is the Euler gamma function. Note that for $a \to 0$, which corresponds to a single-step electron density profile, relations (23) and (24) take the form

$$\tilde{E}_{\mathrm{t}\Omega} = \frac{2K(\Omega)}{K(\Omega)+p(\Omega)}\tilde{E}_{0\Omega}, \quad \tilde{E}_{\mathrm{r}\Omega} = \frac{K(\Omega)-p(\Omega)}{K(\Omega)+p(\Omega)}\tilde{E}_{0\Omega}. \qquad (25)$$

Fig. 3 shows the dependences of conversion coefficients of an incident-pulse frequency component ω to the delayed pulse $[R_{\mathrm{s}}(\omega_{\mathrm{r}}^{\mathrm{s}}) = I_{\mathrm{r}}^{\mathrm{s}}[\omega_{\mathrm{r}}^{\mathrm{s}}(\omega)]/I(\omega)]$ and to the pulse $[T(\omega_{\mathrm{t}}) = I_{\mathrm{t}}[\omega_{\mathrm{t}}(\omega)]/I(\omega)]$ transmitted through the ionisation front obtained from expressions (23)–(25) for $\omega_{\mathrm{p\,max}}^2/\omega_0^2 = 0.1$, $\lambda_0 = 0.8$ μm, and $a = 0.9$ μm. Hereafter, we will consider the case of a relatively tenuous gas for which $n_{\mathrm{e\,max}}/n_{\mathrm{c}} \lesssim 0.1$. Then, the conversion coefficient $R_{\mathrm{b}}(\omega_{\mathrm{r}}^{\mathrm{b}}) = I_{\mathrm{r}}^{\mathrm{b}}[\omega_{\mathrm{r}}^{\mathrm{b}}(\omega)]/I(\omega)$ to the backward reflected pulse proves to be low everywhere, except a small vicinity of the point $\omega = \omega_{\min}$. The spectral components of the weak pulse near $\omega = \omega_{\min}$ are reflected from the travelling ionisation front with frequencies close to the frequency $\omega_{\mathrm{p\,max}}$. The maximum conversion coefficient to the backward reflected component is achieved when the ionisation front represents a step. In the vicinity of $\omega_{\mathrm{r}}^{\mathrm{b}} = \omega_{\mathrm{p\,max}}$, we have

$$R_{\mathrm{b}}(\omega_{\mathrm{r}}^{\mathrm{b}}) \approx \frac{V}{c}\left(1+\frac{V^2}{c^2}\right)\left(1+\frac{V}{c}\right)^{-4}\left(\frac{2\omega_{\mathrm{p\,max}}}{\omega_{\mathrm{r}}^{\mathrm{b}} - \omega_{\mathrm{p\,max}}}\right)^{1/2}.$$

The conversion coefficient $R_{\mathrm{s}}(\omega_{\mathrm{r}}^{\mathrm{s}})$ to the delayed pulse behaves similarly in the vicinity of $\omega_{\mathrm{r}}^{\mathrm{s}} = \omega_{\mathrm{p\,max}}$, as one can see from Fig. 3 for low $\omega_{\mathrm{r}}^{\mathrm{s}}$ ($\omega_{\mathrm{p\,max}} \approx 0.316\,\omega_0$).

One can also see from Fig. 3 that the dependence of conversion coefficients to the delayed pulse and to pulse transmitted through the ionisation front on the corresponding frequencies $\omega_{\mathrm{r}}^{\mathrm{s}}$ and ω_{t} substantially depends on the shape of ionisation front. The highest conversion coefficient (to the transmitted pulse) is achieved with increasing frequency at a more smooth ionisation front. To understand the reason for this difference, we consider other possible shapes of the ionisation front.

4.2 Linearly polarised pulse

When the ionising laser pulse is linearly polarised, the electron density profile has the form of steps of length $\pi V/\omega_0$ (see Fig. 2 and also, for instance, Ref. [16]). We

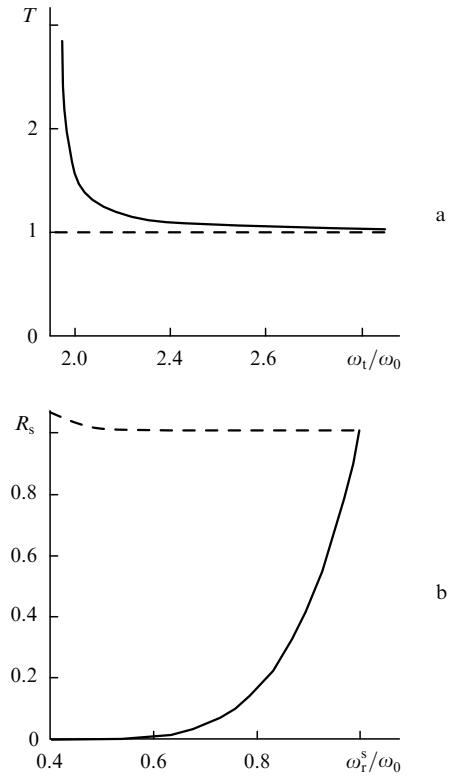

Figure 3. Dependences of the conversion coefficients $T(\omega_{\mathrm{t}})$ (a) and $R_{\mathrm{s}}(\omega_{\mathrm{r}}^{\mathrm{s}})$ (b) obtained from expressions (23) and (24) for the density profile (21) (solid curves) and from expressions (25) for a single step (dashed curves) for $\omega_{\mathrm{p\,max}}^2/\omega_0^2 = 0.1, \lambda_0 = 0.8$ μm, and $a = 0.9$ μm ($\omega_{\mathrm{t\,min}} = \omega_{\mathrm{t}}(\omega = o_0) \approx 1.95\omega_0, T(\omega_{\mathrm{t\,min}}) \approx 2.86$).

approximate this profile, which is generally multi-step, by the expression:

$$n_{\mathrm{e}}(\zeta) = n_{\mathrm{e\,max}}\theta(-\zeta) + \sum_{l=1}^{N} n_{\mathrm{e}l}\theta(l\pi V/\omega_0 - \zeta)\,\theta[\zeta - (l-1)\pi V/\omega_0], \qquad (26)$$

where $n_{\mathrm{e}l}$ (lower than $n_{\mathrm{e\,max}}$) are the electron densities at the steps that decrease with l, and $\theta(u)$ is the Heaviside step function. For $N = 1$ (a two-step profile), the solutions of (3), (4) for $\tilde{E}_{\mathrm{t}\Omega}$ and $\tilde{E}_{\mathrm{r}\Omega}$ have the form

$$\tilde{E}_{\mathrm{t}\Omega} = \frac{2K(\Omega)K_1(\Omega)\exp[-\mathrm{i}\pi p(\Omega)V/\omega_0]}{K_1(\Omega)[K(\Omega)+p(\Omega)]\cos\varphi - \mathrm{i}[K_1^2(\Omega)+p(\Omega)K(\Omega)]\sin\varphi}\tilde{E}_{0\Omega}, \qquad (27)$$

$$\tilde{E}_{\mathrm{r}\Omega} = \frac{K_1(\Omega)[K(\Omega)-p(\Omega)]\cos\varphi + \mathrm{i}[K_1^2(\Omega)-p(\Omega)K(\Omega)]\sin\varphi}{K_1(\Omega)[K(\Omega)+p(\Omega)]\cos\varphi - \mathrm{i}[K_1^2(\Omega)+p(\Omega)K(\Omega)]\sin\varphi}\tilde{E}_{0\Omega}, \qquad (28)$$

where

$$K_1(\Omega) = \left[\frac{\Omega^2}{c^2}\left(1-\frac{V^2}{c^2}\right)^{-2} - k_{\mathrm{p1}}^2\left(1-\frac{V^2}{c^2}\right)^{-1}\right]^{1/2};$$

$$k_{\mathrm{p1}}^2 = 4\pi e^2 n_{\mathrm{e1}}/(mc^2); \quad \varphi = \pi K_1(\Omega)V/\omega_0.$$

Fig. 4 shows the dependences of the coefficients of conversion of an incident-pulse frequency component ω to the delayed pulse $[R_s(\omega_r^s)]$ and to the pulse transmitted through the ionisation front $[T(\omega_t)]$, which were obtained from expressions (27) and (28) for $\omega_{p\max}^2/\omega_0^2 = 0.1$, $\lambda_0 = 0.8$ μm, and $n_{e1} = n_{e\max}/2$. One can see that the behaviour of conversion coefficients in the presence of an 'intermediate' step with the density n_{e1} is significantly different from their behaviour in the case of a sharp, single-step profile of the electron density. In the delayed-pulse spectrum R_s there appear peaks related to the rereflection of electromagnetic waves between the two steps.

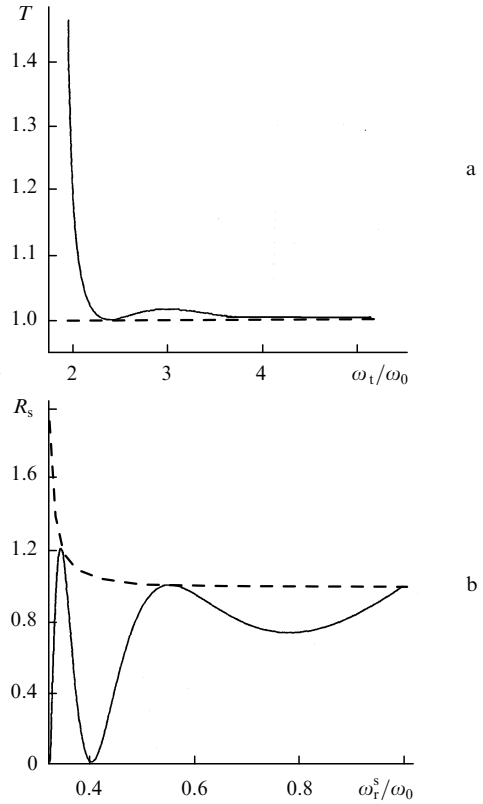

Figure 4. Dependences of the conversion coefficients $T(\omega_t)$ (a) and $R_s(\omega_r^s)$ (b) obtained from expressions (27) and (28) for a two-step profile (26) (solid curves) and from expressions (25) for a single step (dashed curves) for $\omega_{p\max}^2/\omega_0^2 = 0.1$, $\lambda_0 = 0.8$ μm, and $n_{e1} = n_{e\max}/2$.

The duration of interaction between the weak pulse and the ionisation front becomes longer upon such repeated reflection, as if there occurs a capture of electromagnetic radiation. In this case, the electromagnetic waves slowed down at the first step (with the density n_{e1}) are reflected forward (in the direction of front propagation) by the rear step (with the density $n_{e\max}$). This rereflection results in the decrease in the conversion coefficient to the delayed pulse and in the increase in the conversion coefficient $T(\omega_t)$ to the pulse with an increased frequency (see Fig. 4). This trend in variations in the conversion coefficients is also retained with increasing the number of steps (Fig. 5). Note that the increase in the number of steps accompanied by a simultaneous decrease in their height brings the density profile closer to the smooth profile at which the conversion to the delayed pulse is suppressed compared to the conversion to the transmitted pulse (see Fig. 3).

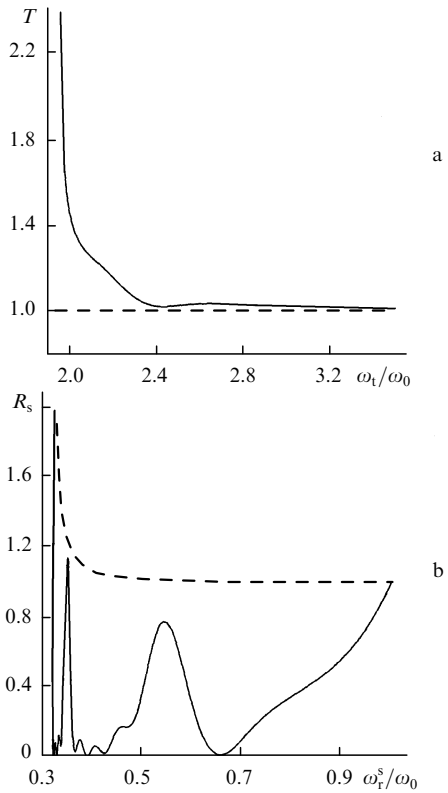

Figure 5. Dependences of the conversion coefficients $T(\omega_t)$ (a) and $R_s(\omega_r^s)$ (b) obtained from expressions (27) and (28) for a five-step profile (26) (solid curves) and from expressions (25) for a single step (dashed curves) for $\omega_{p\max}^2/\omega_0^2 = 0.1$, $\lambda_0 = 0.8$ μm, and $n_{el} = (5-l)n_{e\max}/5$ $(l = 1, \ldots, 5)$.

5. Energy conservation law for spectral intensity densities

The conversion coefficient to the pulse with higher frequencies (to the transmitted pulse) turns out to be higher than unity (see Figs 3–5). This result should be specified from the viewpoint of the energy conservation law. To show that the total energy of electromagnetic radiation is lower than the total energy of the weak pulse, we rewrite expression (19) in the differential form:

$$I(\omega)\delta\omega = I_t(\omega_t)\delta\omega_t + I_r^b(\omega_r^b)\delta\omega_r^b + I_r^s(\omega_r^s)\delta\omega_r^s + \delta R(\omega),$$

where $\delta R(\omega)$ is the term related to the residual electron energy. From this, we obtain

$$1 - T_t(\omega_t)\frac{\delta\omega_t}{\delta\omega} - R_r^b(\omega_r^b)\frac{\delta\omega_r^b}{\delta\omega} - R_r^s(\omega_r^s)\frac{\delta\omega_r^s}{\delta\omega} \equiv \Delta(\omega) = \frac{\delta R(\omega)}{\delta\omega}. \quad (29)$$

This relation represents the energy conservation law for the conversion coefficients. Fig. 6 shows the dependence $\Delta(\omega)$ (29) in the case of a five-step electron density profile (26) and the same parameters as in Fig. 5. The positive values of Δ prove the existence of energy losses of the electromagnetic pulse upon its interaction with the travelling ionisation front.

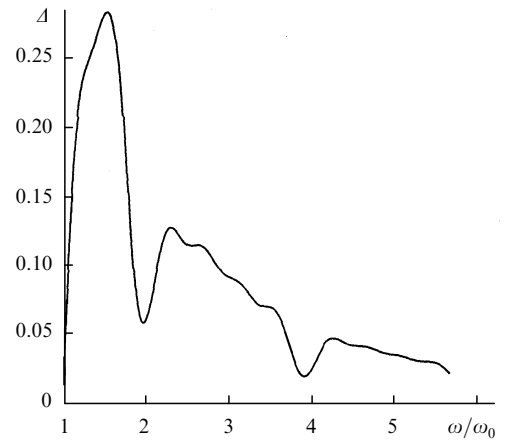

Figure 6. Dependence $\Delta(\omega)$ (29) obtained for a five-step profile (26) for $\omega_{\mathrm{p}\max}^2/\omega_0^2 = 0.1$, $\lambda_0 = 0.8$ μm, and $n_{el} = (5-l)n_{\mathrm{e}\max}/5$ $(l = 1, \ldots, 5)$.

6. Conclusions

Therefore, a weak electromagnetic pulse interacting with a copropagating ionisation front travelling with the velocity $V = c[\varepsilon(\omega_0)]^{1/2}$ generally splits into three pulses: (1) a pulse transmitted through the front, the frequencies of each of its components being increased; (2) a delayed pulse, which propagates through the ionised gas in the same direction as the ionisation front, lags behind it, and has frequencies lower than ω_0; and (3) the reflected pulse, which propagates in the direction opposite to the propagation direction of the ionisation front.

In the region of the extended ionisation front, the electromagnetic radiation is captured resulting in the suppression of the coefficient of intensity conversion to the delayed pulse (of a lower frequency) compared to the conversion coefficient to the pulse (of a higher frequency) transmitted through the front (see, for instance, Fig. 3). A part of the electromagnetic energy is converted to the residual electron energy, which is described by the energy conservation law (29) formulated for the intensities.

According to the above discussion, the propagation conditions for the delayed (with a frequency lower than ω_0) and transmitted (with a frequency higher than ω_0) pulses are significantly different: the low-frequency pulse propagates through an ionised gas, while the high-frequency pulse through a neutral one. As a result, to determine the spectrum of laser radiation transmitted through the gas being ionised, the three-dimensional dynamics of electromagnetic pulse propagation should be considered, because the low-frequency pulse is to a greater extent subjected to the ionisation refraction. The latter circumstance may be responsible for observation in the experiments [12] of only the blue shift of the spectrum of laser radiation transmitted through the gas being ionised, whereas in the one-dimensional calculations [12] a red satellite was also observed.

Acknowledgements. This work was partly supported by the Russian Foundation for Basic Research (Grant No. 01-02-16723).

References

1. Semenova V I *Izv. Vyssh. Uchebn. Zaved. Radiofiz.* **10** 1077 (1967)
2. Semenova V I *Izv. Vyssh. Uchebn. Zaved. Radiofiz.* **15** 647 (1972)
3. Semenova V I *Izv. Vyssh. Uchebn. Zaved. Radiofiz.* **15** 1793 (1972)
4. Lampe M, Ott E, Walker J H *Phys. Fluids* **21** 42 (1978)
5. Wilks S C, Dawson J M, Mori W B, Katsouleas T, Jones M E *Phys. Rev. Lett.* **62** 2600 (1989)
6. Gil'denburg V B, Kim A V, Sergeev A M *Pis'ma Zh. Eksp. Teor. Fiz.* **51** 91 (1990) [*JETP Lett.* **51** 104 (1990)]
7. Esarey E, Ting A, Sprangle P *Phys. Rev. A* **42** 3526 (1990)
8. Mironov V A, Sergeev A M, Vanin E V, Brodin G *Phys. Rev. A* **42** 4862 (1990)
9. Wood W M, Siders C W, Downer M C *Phys. Rev. Lett.* **67** 3523 (1991)
10. Gil'denburg V B, Pozdnyakova V T, Shereshevskii I A *Phys. Lett. A* **203** 214 (1995)
11. Oliveira e Silva L, Mendonca J T *IEEE Trans. Plasma Sci.* **24** 316 (1996)
12. Koga J T, Naumova N, Kando M, Tsintsadze L N, et al. *Phys. Plasmas* **7** 5223 (2000)
13. Siders C W, Le Blanc S P, Babine A, Stepanov A, et al. *IEEE Trans. Plasma Sci.* **24** 301 (1996)
14. Chegotov M V *Fiz. Plazmy* **26** 940 (2000) [*Plasma Phys. Reports* **26** 881 (2000)]
15. *Handbook of Mathematical Functions* M Abramowitz, I A Stegun (Eds) (New York: Dover, 1965)
16. Andreev N E, Chegotov M V, Veisman M E *IEEE Trans. Plasma Sci.* **28** 1098 (2000)